



Effect of solvent on the morphological and optical properties of CuO nanoparticles prepared by simple sol-gel process

N. Zayyoun^{1*}, B. Jaber², L. Laânab¹, E. Ntsoenzok³ and R. Bekkari¹

¹⁾ LCS, Faculty of Sciences, Mohammed V University, Rabat, Morocco.

²⁾ Materials Science Platform, UATRS division, CNRST, Rabat, Morocco.

³⁾ CNRS, CEMTHI UPR3079, Site Cyclotron, 3A rue de la Férolerie, 45071 Orléans, France

Received 19 Oct 2015, Revised 19 Mar 2016, Accepted 23 Mar 2016

*Corresponding author: najouazayyoun@gmail.com

Abstract

CuO nanoparticles with different morphologies were successfully synthesized by the sol-gel method through the reduction of copper acetate in different solvents. The influence of the kind of solvent on the structural, morphological and optical properties of nanoparticles was investigated. X-ray diffraction studies showed that the nanoparticles are monoclinic in nature without secondary phases and their size depends greatly on the nature of the solvent. TEM images indicate that the obtained CuO nanoparticles are predominantly of spherical shape, with sizes in the quantum dots range (from 4 to 9.5nm). The smallest particles were obtained when using the ethanol as solvent. A net blue shift in the fundamental direct gap energy (from 4.2 to 4.9eV), attributed to the quantum confinement effect, is observed in the optical analysis when the particles size decreases. Moreover, the purity of the obtained NPs was confirmed through the Raman spectroscopy characterizations, which show the absence of any secondary phases. The downshifted peaks is attributed to the size effect.

Keywords: CuO, nanoparticles, sol-gel, characterization, quantum confinement

1. Introduction

Inorganic nanostructures with well-defined morphologies having outstanding properties and potential applications have received considerable attention in recent years. Metal oxide nanoparticles (MOs) are very important in inorganic material research to develop different practical applications. These nanoparticles have unique chemical and physical properties [1-3] depends strongly on their shape, size, composition and structure [4-6].

Among all the MOs, CuO nanoparticles are the most studied materials due to its interesting properties as a p-type semiconductor with the possibility of a large band gap variation. In fact, the reported gap energy values of this material are ranging from 1.2eV, for the bulk CuO, to 4.13eV for 10 nm quantum dots [7-9]. Moreover, because of their high solar absorbance and low thermal emittance [10], CuO NPs are very attractive materials for the fabrication of the solar cells. CuO nanostructures are also relevant candidates in various other applications including gas sensors [11], anodes in battery [12], nanofluid [13], photodetectors [14], energetic materials [15], field emissions [16], supercapacitors [17], photocatalysis [18], magnetic storage media [19] and antibacterial materials [20].

During the past few years, various methods were used to synthesize the CuO NPs including thermal oxidation of Copper in air [21], solvothermal [22], sol-gel [23], microwave irradiation [24], hydrothermal [25] and sonochemical method [26]. From all the above synthesis process, it seems to be very difficult to obtain a pure crystallographic CuO material without adding many stabilizing agents. In fact, as it was reported[27], the elaboration of CuO NPs is usually accompanied by the presence of secondary phases like Cu₂O or Cu(OH)₂. For that, the challenge taken up in this work is to synthesize pure CuO NPs, in the quantum dot range, using the low

cost sol-gel method without adding any stabilizing agent. This method can co-synthesize simultaneously and accurately two or more materials and control the microstructural, physical and chemical properties of the final product. Also, as it can be deduced from this work, when the synthesis parameters are well optimized, the sol-gel method can produce pure materials at ultra-low temperatures. In this framework, the present paper aims as well to study the effect of the solvent nature on the microstructural and optical properties of the as-synthesized CuO NPs.

2. Experimental details

2.1. Preparation of CuO NPs

Copper (II) acetate monohydrate ($\text{Cu}(\text{CH}_3\text{COO})_2 \cdot \text{H}_2\text{O}$), water, ethanol, propanol and NaOH, of analytical grade purity, are used in the experiments. In order to elaborate the CuO NPs by sol-gel process, 1.98 g of ($\text{Cu}(\text{CH}_3\text{COO})_2 \cdot \text{H}_2\text{O}$) is dissolved and stirred for 1 hour in 100 ml of water to get a homogenous solution. Then 0.8 M of NaOH is added to this solution maintained at 60°C under constant stirring during 2 hours. Finally the obtained black precipitate is centrifuged (14000 rpm) and washed twice with distilled water and once with absolute ethanol to remove all kinds of impurities, then dried at 50°C . In order to evaluate the effect of the solvent on the structural, morphological and optical properties, we use also ethanol and propanol instead of water in the process. For all reactions, the copper acetate and NaOH concentrations, temperature and time of the reaction are maintained constant.

2.2. Characterization

The obtained powder is characterized by X Ray Diffraction using the Panalytical XPERT-PRO powder diffractometer with the $\text{Cu-K}\alpha$ radiation. The morphology of the prepared CuO nanoparticles is carried out using the FEI Transmission Electron Microscopy (TEM, Tecnai G2 12 TWIN, 120KV) with a LaB_6 filament. The UV-Visible absorption spectra have been recorded by means of the UV-Visible Perkin Elmer spectrophotometer (Lambda 900). To confirm the chemical purity of the obtained material, additional Raman analysis is performed via a Raman spectrometer with a 532 nm laser source.

3. Results and discussion

3.1. Structural properties

Figure 1 displays the X-Ray diffraction pattern of the synthesized CuO NPs using propanol, water and ethanol as solvents. In the three cases, the two main observed reflection peaks ($2\theta = 35.6^\circ$ and $2\theta = 38.8^\circ$) are ascribed to the (002) and (111) reflections in the CuO monoclinic crystal phase, according to the JCPDS card N^o: 048-1548.

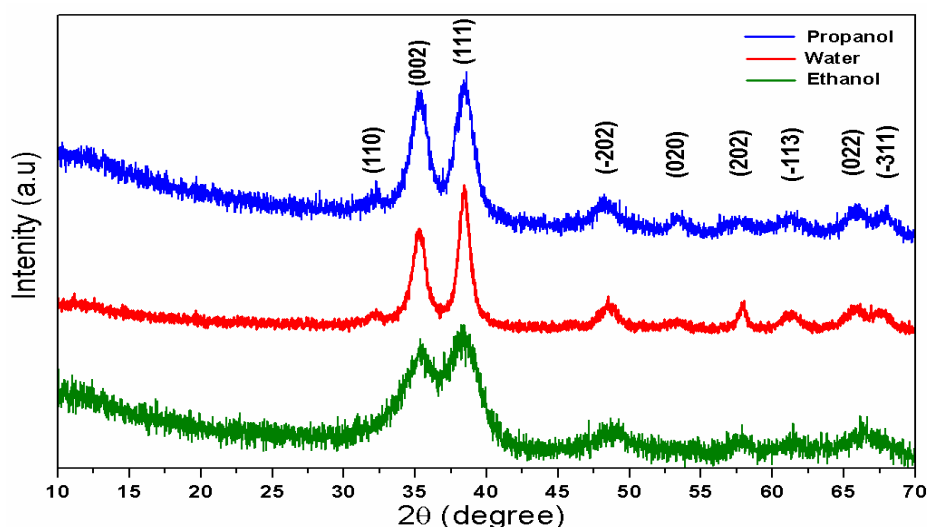


Figure 1: X-Ray Diffraction pattern of CuO NPs, synthesized by sol-gel in different solvents: propanol, water and ethanol.

All the other peaks, with minus intensities, are also well matched with this monoclinic phase of CuO. Meanwhile, no secondary phases such as Cu, Cu₂O or Cu(OH)₂ are detected in the XRD pattern. Consequently, these XRD results confirm the synthesis of pure and well crystalline CuO NPs and are well consistent with previously reported works [28, 29]. Furthermore, the diffraction patterns show that all the peaks present a broadening, which depends on the solvent nature. As is reported [9, 30, 31], this broadening has been linked to the crystallite size and the lattice strain.

The average crystallite sizes of CuO NPs calculated by Scherrer formula [30] are 13.4 nm, 11.8 nm and 9.4 nm when using propanol, water and ethanol respectively. This result is in good agreement with the observed 2θ shift towards the higher angles when using ethanol as solvent.

3.1. Morphological studies

Typical TEM images and size distribution of the as prepared CuO nanoparticles in different solvents are presented in Figure 2. It's clear that the morphology and the size of CuO nanoparticles depend strongly on the solvent nature. The TEM micrographs confirm also the tendency in the evolution of the CuONPs average size as revealed by the XRD results.

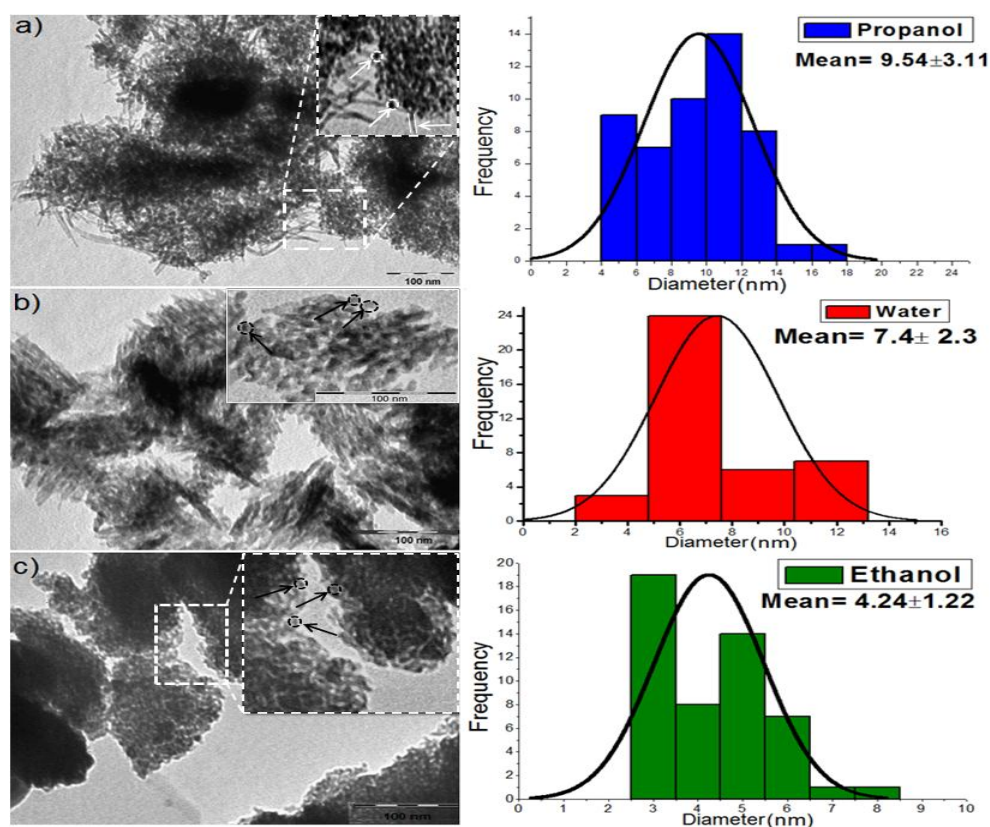


Figure 2: TEM images and particle size distribution of the CuO NPs prepared by sol-gel in: a) propanol, b) water and c) ethanol.

The powder prepared in propanol consists of a mixture of needle-shaped and small spherical particles having an average diameter of 9.5 nm (Fig.2a). Meanwhile, the NPs prepared in water are spherical and aligned along the c-axis direction with an average diameter of about 7 nm (Fig.2b). However, in the case of ethanol (Fig.2c), only spherical NPs with narrow sizes distribution (about 4nm) are observed. These results show that the morphology of the CuO NPs synthesized in alcoholic solvents depends strongly upon the chain length of the alcohol molecule. It was reported [32] that the chain length plays a significant role in orienting the nanocrystal growth and in stabilizing specific crystallographic planes. Therefore, in the case of propanol which has the longest chain, the particles grow in nano-needles shape as confirmed by TEM observations. By contrast, when the

alcoholic chain becomes short (water and ethanol), no oriented growth occurs and then only spherical NPs are formed.

3.2. Optical properties

The absorption spectra of CuO nanoparticles synthesized by sol-gel using water, ethanol and propanol as solvents are shown in Figure 3. All the samples exhibit a maximum absorption peak at about 350 nm.

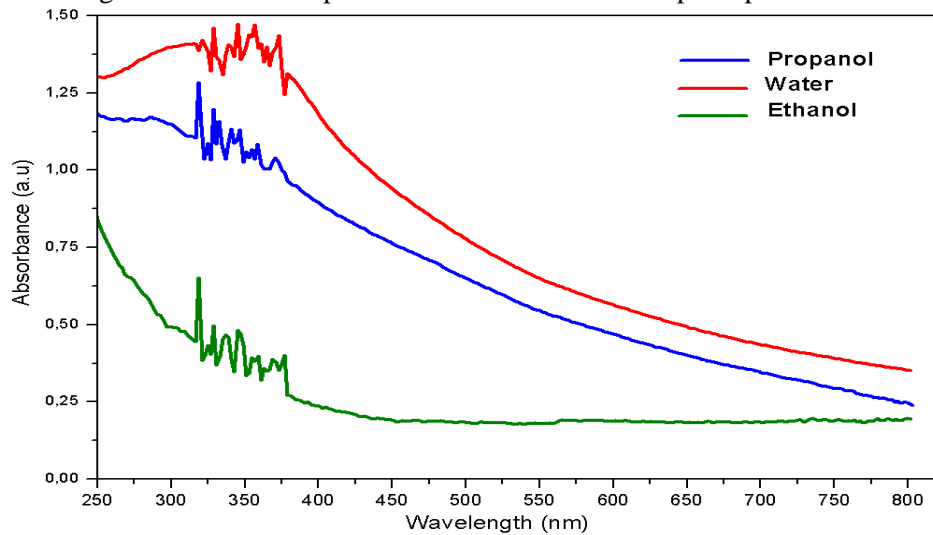


Figure 3: UV-Vis spectra of CuO nanoparticles synthesized by sol-gel in different solvents.

To estimate the band gap of CuO nanoparticles from the absorption spectra we use the relation (Willardson and Beer) given below:

$$(\alpha h\nu) = A(h\nu - E_g)^n$$

where E_g is the gap energy of the material, ν is the frequency of the incident radiation, h is Planck's constant, α is the absorption coefficient in cm^{-1} , A is a constant related to the material and the matrix element of the transition, and n is a coefficient depending on the nature of the transition ($n = 1/2$ for the direct allowed transition or 2 for an indirect transition). The absorption coefficient is obtained using the relation $\alpha \cdot d = \ln(1/T)$, where the transmittance T is calculated from the measured absorbance using the Beer-Lambert law, $B = -\log_{10}(T)$; d represents the path length of the wave in centimeter (1cm). To obtain the absorption onset, $(\alpha h\nu)^2$ is plotted against energy $h\nu$. Extrapolation of the linear part until its intersection with the $h\nu$ axis provides the value of E_g (Fig. 4).

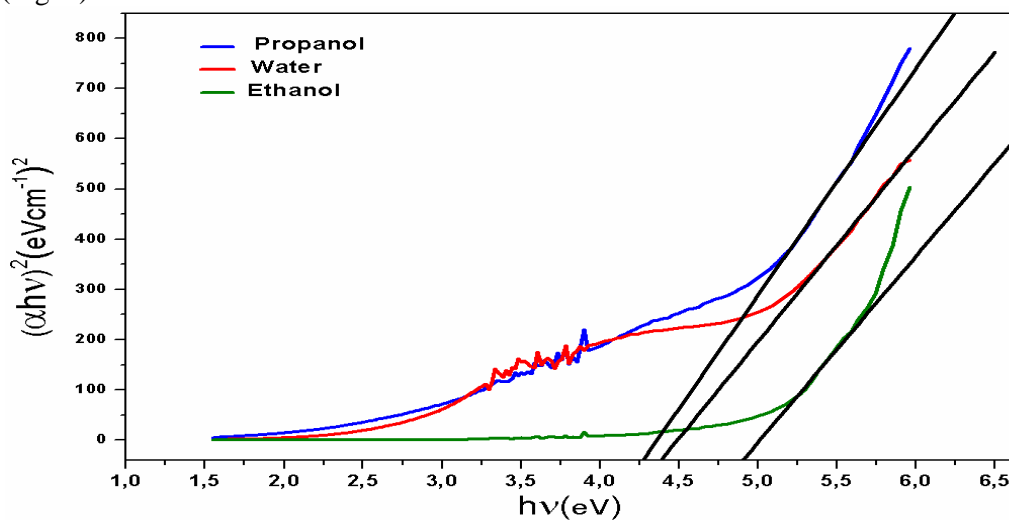


Figure 4: The plot of $(\alpha h\nu)^2$ versus photon energy ($h\nu$) for CuO nanoparticles prepared in different solvents.

The obtained values of direct band gap are 4.2 eV, 4.3eV and 4.9eV for propanol, water and ethanol respectively. Figure 5 shows the variation of the measured gap energy with crystallite diameter of CuO nanoparticles prepared by sol-gel in different solvents. From these graphs, it's clear that the direct gap energy increases with decreasing particle diameter. The highest gap energy (4.9eV) value is obtained for the smallest particle size (4.2 nm). The gap energy values obtained for the CuO NPs in this work are in the range of those reported by the literature [8]. A blue shift in the direct gap energy is observed as the particles diameter is reduced. This phenomenon, known as the exciton Bohr radius, corresponds to a principal shift in optical and electronic properties. Such a blue shift has been reported in the literature for CuO quantum dots [8, 33] when the particles size are ranged from 7 to 30 nm. The CuO nanoparticles synthesized in this work are therefore within the strong confinement regime.

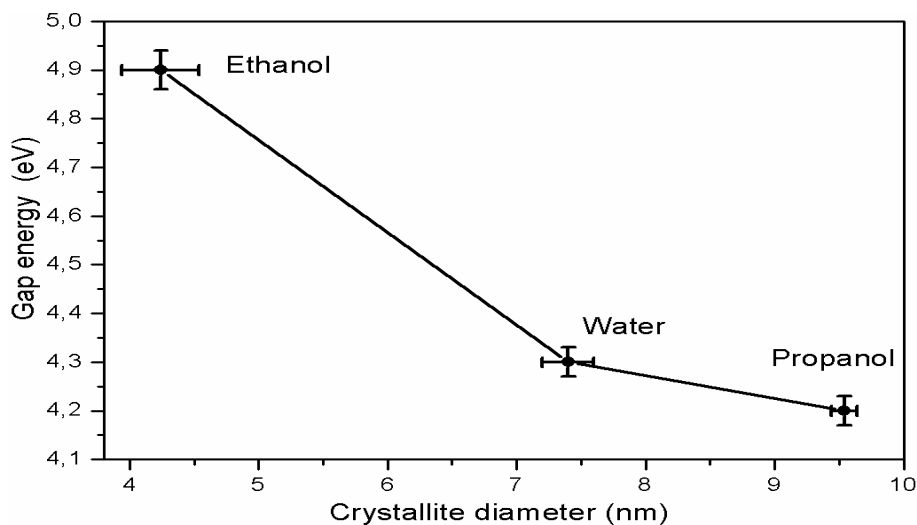


Figure 5: Direct band gap variation with crystallite diameter of the prepared CuO nanoparticles.

3.3. Raman analysis

Figure 6 shows the Raman spectrum of CuO nanoparticles synthesized by the sol-gel method using water as solvent. CuO has a monoclinic structure with space group C_{2h}^6 and two molecules per primitive unit cell [34]. One can find the zone center Raman active normal modes $\Gamma_{RA} = 4Au + 5Bu + Ag + 2Bg$. There are three acoustic modes (Au + 2Bu), six infrared active modes (3Au + 3Bg), and three Raman active modes (Ag + 2Bg).

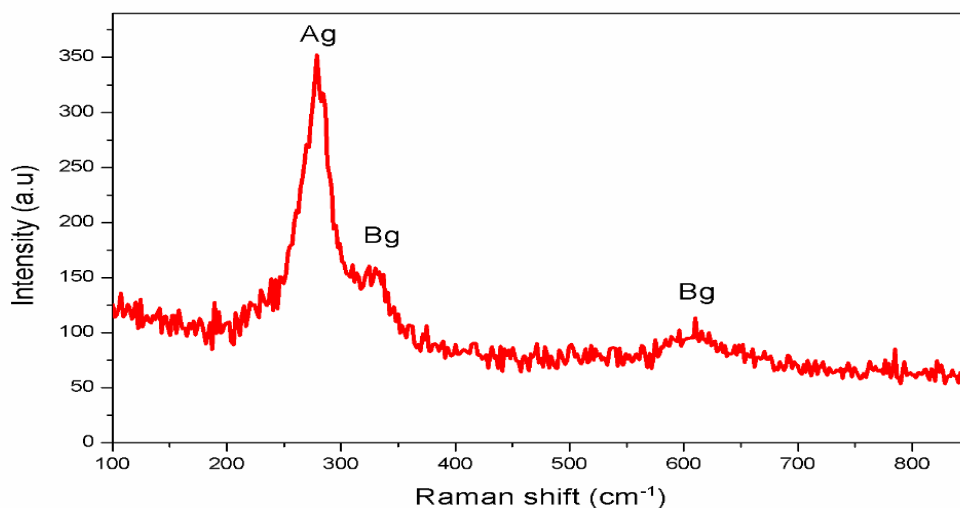


Figure 6: Raman spectrum of CuO nanoparticles synthesized in water as solvent.

The Raman spectrum (Fig.6) of the CuO nanoparticles exhibit three peaks at 280cm^{-1} , 329cm^{-1} and 613cm^{-1} . Compared with the vibrational spectra of CuO single crystal [35, 36], the obtained Raman peaks are downshifted due to the size effect [35]. We attribute the peak at 280cm^{-1} to the Ag mode and the peaks at 329cm^{-1} , 613cm^{-1} to the Bg modes, which are consistent with previous works [37, 38]. This result shows obviously that pure single phase CuO nanoparticles are formed in the above experimental conditions.

Conclusion

Pure crystallographic CuO nanoparticles, ranging from 4 to 10 nm, were synthesized by sol-gel method, without introducing any stabilizing agent in the process. The effect of solvent on the structure, morphology and optical properties of CuO nanoparticles was studied. Pure monoclinic CuO nanoparticles, with single phase, were identified by XRD and Raman techniques. However, TEM micrographs reveal that the morphology and the size of the synthesized NPs change according to the solvent. In fact, this morphology varies from spherical (4nm) to needle-shaped (9.5 nm) when varying the solvent from ethanol to propanol respectively. The observed change is attributed to the variation of the length of the alcoholic chain. Furthermore, the measured direct band gap values for the synthesized CuO NPs indicated a blue shift due to the quantum confinement effect.

Acknowledgement - The authors would like to thank Pr Adnan Mlayah from CEMES/CNRS, Toulouse for Raman measurements.

References

1. Tiwari J. N., Tiwari R. N., Kim K. S., *Prog. Mater. Sci.* 57 (2012) 724.
2. Spencer M. J. S., *Prog. Mater. Sci.* 57 (2012) 437.
3. Barth S., H-Ramirez F., et al., *Prog. Mater. Sci.* 55 (2010) 563.
4. Chen X., Mao S. S., *Chem. Rev.* 107 (2007) 2891.
5. Park J., Joo J., et al., *Angew. Chem. Int. Ed.* 46 (2007) 4630.
6. Zheng H., Ou J.Z., et al., *Adv. Funct. Mater.* 21 (2011) 2175.
7. Ogwu A.A., Darma T.H., Bouquerel E., *J. Achiev. Mater. Manufact. Eng.* 24 (2007) 172.
8. Borgohain K., Mahamuni S., *J. Mater. Res.* 17 (2002) 1220.
9. Mallick P., Sahu S., *Nanoscience and Nanotechnology* 2 (2012) 71.
10. Kislyuk V.V., Dimitriev O.P., *J. Nanosci. Nanotechnol.* 8 (2008) 131.
11. Choi K.J., Jang H.W., *Sensors* 10 (2010) 4083.
12. Song M-K., Park S., et al., *Mater. Sci. Engineering: R: Reports* 72 (2011) 203.
13. Sahin B., Manay E., Akyurek E.F., *J. Nano.* 2015 (2015) 1.
14. Wang S.B., Hsiao C.H., et al., *Sen. Actuat. A: Phys.* 171 (2011) 207.
15. Rossi C., Zhang K.D., et al., *J. Microelectromech. Syst.* 16(2007) 919.
16. Zhu Y.W., Yu T., et al., *Nanotechnology* 16(2005) 88.
17. Zhang X., Shi W., et al., *ACS Nano*. 5 (2011) 2013.
18. Kim S.H., Umar A., et al., *Mater. Letters* 156 (2015) 138.
19. Kumar R.V., Diamant Y., Gedanken A., *Chem. Mater.* 12 (2000) 2301.
20. Azimirad R., Safa S., *Synthesis and Reactivity in Inorganic, Metal-Organic, and Nano-Metal Chemistry* 44 (2014) 798.
21. Kumar R. V., Elgamiel R., et al., *Langmuir* 17 (2001) 1406.
22. Wang H., Xu J-Z., et al., *J. Cryst. Growth* 244 (2002) 88.

23. Zhang Q., Li Y., et al., *J. Mater. Sci. Lett.* 20 (2001) 925.
24. Fan H., Yang L., et al., *Nanotechnology* 15 (2004) 37.
25. Azimirad R., Safa S., Akhavan O., *Acta Physi. Polo. A* 127 (2015) 1727
26. S. Sonia S., Jayram N. D., et al., *Super. latt. Micro.* 66 (2014) 1.
27. Nikam A.V., Arulkashmir A., et al., *Cryst. Growth Des.* 14 (2014) 4329.
28. Langford J.I., Louer D., *J. Appl. Crystallogr.* 24 (1991) 149.
29. Abaker M., Umar A., et al., *J. Phys. D: Appl. Phys.* 44 (2011) 155.
30. Cullity B.D., *Elements of X-RAY DIFFRACTION*, Addison-Wesley Publishing Company, (1978).
31. Bindu P., Thomas S., *J. Theor. Appl. Phys.* 8 (2014) 123.
32. Kumar P., Mittal K.L., *Handbook of Microemulsion Science and Technology*, Marcel Dekker, (1999).
33. Schmid G., *Nanoparticles: From Theory to Application*, Wiley-VCH, (2004).
34. Narang S.N., Kartha V.B., Patel N.D., *Physica C: Superconductivity* 204 (1992) 8.
35. Goldstein H.F., Kim D.S., et al., *Phys. Rev. B* 41(1990) 7192.
36. Irwin, J.C., Chrzanowski J., et al., *Phys. C: Superconductivity* 166 (1990) 456.
37. Xu J. F., Ji. W., et al., *J. Raman Spectrosc.* 30 (1999) 413.
38. Wang W., Liu Z., et al., *Appl. Phys. A* 76 (2003) 417.

(2016) ; <http://www.jmaterenvironsci.com/>